# Can VMD improve the estimate of the muon $g-2$?

M. Benayoun[1)] L. Del Buono B. P. David O. Leitner

LPNHE des Universités Paris VI et VII, IN2P3–CNRS, Paris, 75005, France

**Abstract** We show that a VMD based theoretical input allows for a significantly improved accuracy for the hadronic vacuum polarization of the photon which contributes to the theoretical estimate of the muon $g-2$. We also show that the only experimental piece of information in the $\tau$ decay which cannot be accounted for within this VMD framework is the accepted value for $Br(\tau\to\pi\pi\nu_\tau)$, while the $\tau$ spectum lineshape is in agreement with expectations from $e^+e^-$ annihilations.

**Key words** VMD, isospin symmetry breaking, $g-2$

**PACS** XXXXXXXXXXXXXXXXXXXXX XXXXXXXXXXX XXXXXXXXXXXXXX

## 1 Introduction

The Hidden Local Symmetry (HLS) Model [1, 2] implements the Vector Meson Dominance asssumption within the framework of Effective Lagrangians. The non–anomalous sector of this model covers annihilation channels like $e^+e^-\to\pi^+\pi^-$ or $e^+e^-\to K\overline{K}$ and some important decay channels like $\tau\to\pi\pi\nu_\tau$. The non–anomalous sector can be supplemented with an anomalous sector [3–5], allowing[2)] for $\gamma\gamma$P, $\gamma$PV, PVV, $\gamma$PPP and VPPP couplings. Therefore, annihilation processes like $e^+e^-\to(\pi^0/\eta)\gamma$, or $e^+e^-\to\pi^0\pi^+\pi^-$ can enter the HLS framework as well as all radiative decay processes of the form $V\to P\gamma$ or $P\to\gamma\gamma$ or also processees like $\eta/\eta'\to\pi^+\pi^-\gamma$.

Therefore, the HLS model provides a unified framework valid in the low energy regime up to the $\phi$ mass region. It encompasses most annihilation and decay processes.

However, in order to be confronted with experimental data, the HLS model should be equiped with symmetry breaking mechanisms. Implementing $SU(3)$ breaking is done using a variant [6] of the BKY mechanism [7] in the non–anomalous sector. Breaking of the (nonet) $U(3)$ symmetry for pseudoscalar mesons is also an important issue; it is generated [8] by determinant term Lagrangian pieces [9]. The $SU(3)$ breaking of the anomalous Lagrangian is done following the scheme proposed by [10, 11] supplemented with a vector field renormalization recently justified [12]. This full $SU(3)/U(3)$ breaking of the HLS model, recalled in Ref. [12], has allowed a successfull description of all light meson radiative decays [13, 14].

A consistent treatment of the $e^+e^-\to\pi^+\pi^-$ annihilation and the $\tau\to\pi\pi\nu_\tau$ decay requires an appropriate mechanism for Isospin Symmetry breaking (ISB). This has been defined in Ref. [12] and has improved the description of all the processes listed above (annihilation and decay processes) as shown in Ref. [15, 16].

## 2 How can VMD improve estimates of $g-2$?

Therefore, the HLS model provides a framework able to describe in a unified way an important number of cross sections[3)] with an additional set of decay partial widths, essentially radiative decay modes of vector mesons. These play the major role of constraints in order to determine numerically the parameters of the $SU(3)/U(3)/SU(2)$ breaking scheme.

The decay $\tau\to\pi\pi\nu_\tau$ is nothing but an additional constraint, also subject to ISB effects usually

Received 25 January 2010, Revised 30 March 2010

1) E-mail: benayoun@in2p3.fr

2) From now on P and V denote any pseudoscalar and any vector fields from the basic $SU(3)$ nonets.

3) We will use $e^+e^-\to\pi^+\pi^-$, $e^+e^-\to\pi^0\gamma$, $e^+e^-\to\eta\gamma$ and $e^+e^-\to\pi^0\pi^+\pi^-$. Instead, the $e^+e^-\to K\overline{K}$ cross section will be left aside because of a still misunderstood problem concerning the ratio of two kaon decay modes of the $\phi$ meson[17].

split up into short range [18] and long range [19, 20] (resp. $S_{\rm EW}$ and $G_{\rm EM}(s)$) corrections. These are overall rescaling factors.

Within this unified model [15], all relevant data (already listed) depend on a very few number of fundamental parameters, namely the CKM matrix element $V_{\rm ud}$, the electric charge $e$, the pion decay constant $f_\pi$, the universal vector coupling $g$, the weak interaction coupling $g_2$ and a parameter named $a$, specific of the HLS model [2, 6] and expected close to 2. $V_{\rm ud}$, $f_\pi$, and $g_2$ (related to the Fermi constant $g_2 = 2m_{\rm W}\sqrt{\sqrt{2}G_{\rm F}}$) are accurately known. Therefore, the only fundamental parameters to be fitted from data are $a$ and $g$. The anomalous sector introduces 4 more parameters (named $c_i$ in Ref. [2]) in such a way that only two parameters should be determined by fit [15]: the combination $c_1 - c_2$ and $c_3$.

The $U(3)/SU(3)$ breaking procedure introduces 4 breaking parameters determined by only the radiative decays [12, 15]: $z_{\rm A}$, $z_{\rm V}$, $z_{\rm T}$ and $x$. Some of these have a clear physical meaning. Indeed, $z_{\rm A} = [f_{\rm K}/f_\pi]^2$ is the squared ratio of the kaon and pion decay constants. $x$ is the nonet symmetry breaking parameter, tightly related with the pseudoscalar mixing angle in the octet–singlet basis [12, 14] $\theta_{\rm PS} \simeq -10^\circ$. More important for the present purpose is the ISB breaking scheme which introduces more parameters [12, 15] to be fitted and is sketched below.

Our extended model [15] can provide a global fit to the whole set of data listed above. Stated otherwise, the parameters given above underly a physics content common to a very large number of annihilation and decay channels. Therefore, our overconstrained parametrization of the VMD physics allows for a global overconstrained fit. Then, if these constraints are well accepted by the data, the parameter values and the parameter error covariance matrix returned by the global fit will be defined with high accuracy. This should reflect in better estimates of the various contributions of the photon hadronic vacuum polarization (HVP) to $a_\mu$. For this purpose, one only relies on the description quality of the annihilation cross sections and on the consistency of the various data sets with each other.

The quality of the description reached for each of the various cross sections also gives a hint about the quality of the estimates these allow for $a_\mu$. As stated above, the limit of validity of the HLS model extends to slightly above the $\phi$ mass. However, this $s$ region contributes more than 80% to the numerical value for $a_\mu$ and the corresponding uncertainty is as large as $\simeq 35\%$ of the total $a_\mu$ uncertainty. Therefore, even if limited, the expected improvements may have important consequences concerning the physics of $g-2$.

## 3 Breaking of the isospin symmetry: Vector field mixing

The neutral vector mesons, which enter the HLS Lagrangian – as any other VMD Lagrangian – are the so–called ideal fields $\rho^0_{\rm I}$, $\omega_{\rm I}$ and $\phi_{\rm I}$. At leading (tree) order, these are mass eigenstates with resp. masses $m^2_\rho = m^2_\omega \equiv m^2$ and $m^2_\phi = z_{\rm V} m^2$ ($m^2 = ag^2 f^2_\pi$). However, at one loop order, the Lagrangian piece :

$$\mathcal{L}_1 = \frac{iag}{4z_{\rm A}} \left\{ \left[\rho^0_{\rm I} + \omega_{\rm I} - \sqrt{2} z_{\rm V} \phi_{\rm I}\right] K^- \overleftrightarrow{\partial} K^+ + \left[\rho^0_{\rm I} - \omega_{\rm I} + \sqrt{2} z_{\rm V} \phi_{\rm I}\right] K^0 \overleftrightarrow{\partial} \overline{K}^0 \right\} \quad (1)$$

induces transitions among the ideal vector meson fields $\rho^0_{\rm I}$, $\omega_{\rm I}$ and $\phi_{\rm I}$ through kaon loops[1)]. Therefore, at one loop order, the ideal fields are no longer mass eigenstates and thus do not coincide any longer with the physical $\rho^0$, $\omega$ and $\phi$ fields which, instead, must be mass eigenstates. At one loop order, the squared mass matrix $M^2$ for the field triplet ($\rho^0_{\rm I}$, $\omega_{\rm I}$, $\phi_{\rm I}$) is given by Eq. (12) in Ref. [12] and its eigensystem can be constructed perturbatively. One can define 3 mixing functions [15]: $\alpha(s)$, $\beta(s)$, $\gamma(s)$ which can be considered as complex "angles" and are function of $s$, the squared momentum flowing through the vector meson line. $\alpha(s)$, $\beta(s)$ and $\gamma(s)$ describe resp. the $\rho^0 - \omega$, $\rho^0 - \phi$ and $\omega - \phi$ mixings. These angles [15], functions of the kaon loops and of the pion loop, contain subtraction polynomials to be fitted using experimental data. The relationship between ideal and physical fields can be written in terms of these angles:

$$\begin{pmatrix} \rho^0_{\rm I} \\ \omega_{\rm I} \\ \phi_{\rm I} \end{pmatrix} = \begin{pmatrix} \rho^0 - \alpha(s)\ \omega + \beta(s)\ \phi \\ \omega + \alpha(s)\ \rho^0 + \gamma(s)\ \phi \\ \phi - \beta(s)\ \rho^0 - \gamma(s)\ \omega \end{pmatrix}. \quad (2)$$

Therefore, the vector meson mixing is induced by loop corrections and is thus $s$-dependent. This is the most important feature of our isospin symmetry breaking procedure. This field transformation propagates to the interaction terms. For instance, the Lagrangian piece describing the interaction of a pion pair with

1) Actually, with a more complete Lagrangian, $K^*\overline{K}^*$ and $KK^*$ loops come in complementing the kaon loops along the same lines [12].

vector mesons becomes:

$$\frac{iag}{2}\rho_I^0\pi^-\overleftrightarrow{\partial}\pi^+ \Rightarrow \frac{iag}{2}\left[\rho^0-\alpha(s)\ \omega+\beta(s)\phi\right]\pi^-\overleftrightarrow{\partial}\pi^+, \quad (3)$$

which clearly exhibits the origin of the isospin 1 part of the physically observed $\omega$ and $\phi$ fields. Instead, at this order, the coupling of the $\rho^0$ meson to a pion pair is unchanged.

The $\gamma-V$ transition term is equally important. Using the field transformation given by Eq. (2), one gets :

$$-eagf_\pi^2\left[\rho_I^0+\frac{1}{3}\omega_I-\frac{\sqrt{2}z_V}{3}\phi_I\right]\cdot A \Longrightarrow$$

$$-e\left[f_\rho^\gamma(s)\rho^0+f_\omega^\gamma(s)\ \omega-f_\phi^\gamma(s)\frac{\sqrt{2}z_V}{3}\phi\right]\cdot A, \quad (4)$$

where the $f_V^\gamma(s)=agf_\pi^2[1+\mathcal{O}(\alpha(s),\beta(s),\gamma(s))]$ have well identified correction terms [12, 15]. The electromagnetic field is denoted by $A$.

The most interesting feature here concerns the $\rho$ meson which then gets different transition amplitudes to the $\gamma$ and $W$ fields, One can, indeed, show that the amplitude ratio is:

$$\frac{f_\rho^\gamma}{f_\rho^W}=\left[1+\frac{\alpha(s)}{3}+\frac{\sqrt{2}z_V}{3}\beta(s)\right], \quad (f_\rho^W=agf_\pi^2), \quad (5)$$

where the $s$-dependent terms represent the isospin 0 part of the $\rho^0$ meson inherited from its $\omega_I$ and $\phi_I$ components. This makes different the interaction of the $\rho^0$ and $\rho^\pm$ fields with resp. the $\gamma$ and $W$ gauge fields.

Therefore, our isospin breaking scheme results in physical vector fields which are mixtures of definite isospin components and their exact content is $s$-dependent.

As the $\rho^0$ coupling to a pion pair is unchanged, its propagator looks much like the standard Gounaris–Sakurai parametrization [21] with slightly different conditions to fix its free parameters [12]. Our model differs from other ones, generally used in most experimental papers we quote, because our parametrization of the decay amplitudes for the transition $(\rho/\omega/\phi)\to e^+e^-$ depends on the squared momentum flowing through the vector meson line.

## 4 Sketching the global fit to data

The cross sections for $e^+e^-\to\pi^+\pi^-$, $e^+e^-\to\pi^0\gamma$, $e^+e^-\to\eta\gamma$ and $e^+e^-\to\pi^0\pi^+\pi^-$ have been worked out in [15] together with the expressions for the relevant set of decay partial widths. The expression for the $\tau\to\pi\pi\nu_\tau$ spectrum has been computed in Ref. [12] and can also be found in Ref. [16]. The corresponding formulae have been implemented within a computer code aiming at performing a (simultaneous) global fit to all existing relevant data sets.

All existing $e^+e^-$ annihilation data samples have been considered in the context of our global fit method. For the $\pi^+\pi^-$ final state, this covers the former data sets collected in Ref. [22] and in Ref. [23] and the more recent ones collected at Novosibirsk [24–28]. All existing data sets with the $(\pi^0/\eta)\gamma$ final states have also been considered [29–33].

For the $\pi^0\pi^+\pi^-$ annihilation channel, the main available data sets have been provided by CMD–2 [24, 34, 34–36] and SND [37, 38]. These have been considered along with older data sets [39, 40] ; only the very old data set from [41] has been eliminated because it was not clear how to account precisely for its systematics.

Actually, after analyzing the scale uncertainties claimed for the CMD–2 and SND three pion data sets, we were led [15] to also leave aside the SND data sets [37, 38].

Finally, the $\pi^+\pi^-$ KLOE data set, collected at Frascati using the ISR method and reanalyzed recently [42], has been considered.

Concerning the $\tau\to\pi\pi\nu_\tau$ spectra, we considered those from CLEO [43], ALEPH [44] and BELLE [45]. These data sets will be commented with some details in Section 6.

Full information about the fit properties and qualities can be found in Refs. [12, 15, 16] and are not presented here because of lack of place. Let us only mention that the fits always show very good probabilities.

When this work was started, we thought about using the phase shift data mostly collected in Ref. [46]. However, in view of the poor fit quality reached within global fits [12], we gave up using them. Indeed, we never succeeded in getting better than an average $\chi^2$ per phase shift data point smaller than 2, even if the phase shift lineshape was nicely reproduced (see Fig. 4 in Ref. [12]).

Therefore, our idea is to use the largest possible set of data in a phenomenological framework. This introduces some theoretical prejudice such as the VMD assumption or the analyticity requirement. We became recently aware of another global fit method based on analyticity, unitarity, chiral symmetry and the properties of the Roy Equations [47, 48]. Conceptually, this approach is clearly parent of ours.

The $\pi\pi$ phase shift data from [46] are used as input and a specific modelling of the pion form factor

is based on the Omnès representation with some free parameters to be fixed by fit to the data (essentially $\tau \to \pi\pi\nu_\tau$ spectra and/or $e^+e^- \to \pi\pi$). The published preliminary results look interesting, but the final study is still under way [49].

## 5 Improved estimate of the photon HVP

In order to estimate the various contributions of the photon HVP to $a_\mu$ for $s \leqslant 1$ GeV, we followed a specific procedure :

- Use always all the $e^+e^-$ annihilation data samples essentially collected at Novosibirsk [22–33], [24, 34, 34–36, 39, 40]
- Use always the various partial widths of types VP$\gamma$ and P $\to \gamma\gamma$ as reported in the Review of Particle Properties [50]. These play a crucial role in order to overconstrain our model parameter values.
- Examine the effect of the $\pi^+\pi^-$ KLOE data [42] separately, because the fit properties of this sample are not fully satisfactory.
- Add as further constraints, separately or altogether, the $\tau$ data from C (CLEO [43]), B (BELLE [45]) and/or A (ALEPH [44]), in order to exhibit the specific influence of each.

When comparing with experimental data, we focus in the following on the contribution to $a_\mu$ of the pion loop (i.e. $a_\mu(\pi\pi)$ only), integrated on $\sqrt{s} \in [0.630, 0.958]$ GeV. Indeed, most experimental groups have published estimates for $a_\mu(\pi\pi)$ in this reference energy range. This will allow to compare the results from our fits to external experimental results. As these experimental results are corrected for final state radiation (FSR) effects, we do alike.

In order to validate our approach and illustrate its effect, we have first run our code using each of the data sets from [25], [26] and [28] in isolation, each together with our full set of decay width information (15 pieces). The results derived from the fitted pion form factor data[1)] are reported in the first 3 lines of Table 1 and the errors shown are the total uncertainties, as our procedure combines appropriately [15, 16] statistical and systematic errors.

The radiative corrections to the data sets [25], [26] and [28] have been computed using the same Monte Carlo generator. This is supposed to introduce a common scale uncertainty of 0.4% as this produces bin–to–bin and data set to data set correlations. In order to account for this appropriately, one has considered a merged data set constituted by the data provided in [25], [26] and [28] altogether and treated this merged data set as subject to a scale uncertainty of 0.4%. This turns out to apply to this super data set the standard method recalled in Section 6 of [15] with some details.

Table 1. Our estimates for $10^{10}\ a_\mu(\pi\pi)$ and the corresponding experimental values from resp. [25], [26], [28]. Last line displays the result with KLOE data [42] included. In the last two lines the "experimental values" are averages proposed by [51].

| Data Set | Exp. Value | Reco. Value | Prob. |
|---|---|---|---|
| CMD2 (1995) | $362.1 \pm 2.4 \pm 2.2$ | $362.6 \pm 2.6$ | 54% |
| CMD2 (1998) | $361.5 \pm 1.7 \pm 2.9$ | $362.4 \pm 2.1$ | 56% |
| SND (1998) | $361.0 \pm 1.2 \pm 4.7$ | $361.1 \pm 2.0$ | 99% |
| NSK (all) | $360.2 \pm 3.0_{\rm tot}$ | $361.4 \pm 1.7$ | 57% |
| NSK +KLOE | $358.5 \pm 2.4_{\rm tot}$ | $360.3 \pm 1.5$ | – |

Comparing the experimental information from [25, 26, 28] to our model results, one can check that the central values are consistent with each other and that the (combined) uncertainties are much improved. This is partly due to the 15 decay modes associated each time with the cross section data set considered.

Moreover, the combined fit of these data sets together with the 15 decay partial widths allows for an uncertainty improved by a factor of $\simeq 1.8$ compared with the average value proposed by [51]. The last data column gives the probability of the underlying fit to the pion form factor and the decay data. The fit probability of the SND data clearly reflects a too conservative estimate of their systematics.

KLOE data [42] help in improving estimates at the expense, however, of a poor fit probability, essentially due to a (still) poor control of the systematics within this data set.

Our favorite estimate of $a_\mu(\pi\pi)$ (fourth line in Table 1) is consistent with the newly issued experimental results produced from recent pion form factor data collected using the ISR method by the KLOE Collaboration [52] ($10^{10}\ a_\mu(\pi\pi) = 356.7 \pm 0.4 \pm 3.1$) and by the BaBar Collaboration [53] ($10^{10}\ a_\mu(\pi\pi) = 365.2 \pm 2.7$). However, our estimate for $a_\mu(\pi\pi)$ bears a smaller uncertainty.

1) The results displayed in Table 1 have been recently updated compared to previous in order to wash out the effects of a computer code error.

These two new measurements illustrate the need for a motivated theoretical input in order to take full profit of the new high statistics data sets. Indeed, [53] proposes $10^{10}\ a_\mu(\pi\pi) = 360.8 \pm 2.0_{\rm tot}$ as average of the four experimental values given in Table 1 ([25, 26, 28, 42]) and of the BaBar estimate [53]. Comparing this average with our fit value (last line in Table 1) – which does not use the very recently published BaBar data – is interesting. Indeed, it shows that the increased statistics provided by the ISR method at DAPHNE and BaBar has not allowed a real breakthrough in the accuracy of $a_\mu(\pi\pi)$, because of the systematics specific to each experiment.

Instead, what is illustrated by Table 1 is that an adequate theoretical input – like VMD – may allow sizable improvements, as one ends up with a total uncertainty of 0.47 % of the central value (0.42 % when using also KLOE data). Of course, the relevance of the theoretical input should be (and actually is) reflected by the global fit probabilities.

We do not present here the results obtained by introducing the full $(\pi^0/\eta)\gamma$ and $\pi^+\pi^-\pi^0$ cross section data instead of only the $(\rho/\omega/\phi) \to (\pi^0/\eta)\gamma$ partial widths extracted from them ; this has been analyzed in full details in [16]. Interestingly, they allow to confirm the central values for $a_\mu(\pi\pi)$ displayed in Table 1 without providing a visible improvement for its uncertainty compared to using instead the $(\rho/\omega/\phi) \to (\pi^0/\eta)\gamma$ partial widths.

## 6 Adding the $\tau$ spectra to the fitted data samples

As mentioned in Section 4, we only deal with the CLEO (C) [43], ALEPH (A) [44] and BELLE (B) [45] data sets. The (C) data set is actually the normalized spectrum $1/N{\rm d}N/{\rm d}s$. The absolute normalization for ${\rm d}\Gamma(\tau \to \pi\pi\nu_\tau)/{\rm d}s$ is determined by a multiplicative factor[1)], the branching ratio $Br(\tau \to \pi\pi\nu_\tau)$. Therefore, the CLEO spectrum we use is not sensitive to this branching ratio. As, following the BELLE Collaboration analysis [45], we allow for a rescaling of the B data set, we are only marginally sensitive to $Br(\tau \to \pi\pi\nu_\tau)$ for this data set. Instead, taking into account the high precisison of the $Br(\tau \to \pi\pi\nu_\tau)$ measurement from the ALEPH Collaboration, we have left fixed the absolute normalization of the ALEPH (A) $|F_\pi(s)|^2$ spectrum ; we will nevertheless shortly report on relaxing this constraint.

This way to proceed with B and C is not the usual one. Indeed, usually, the B and C $|F_\pi(s)|^2$ spectra are constructed as their reported normalized spectrum $1/N{\rm d}N/{\rm d}s$ multiplied by the world average value[2)] for $Br(\tau \to \pi\pi\nu_\tau)$ [45, 51].

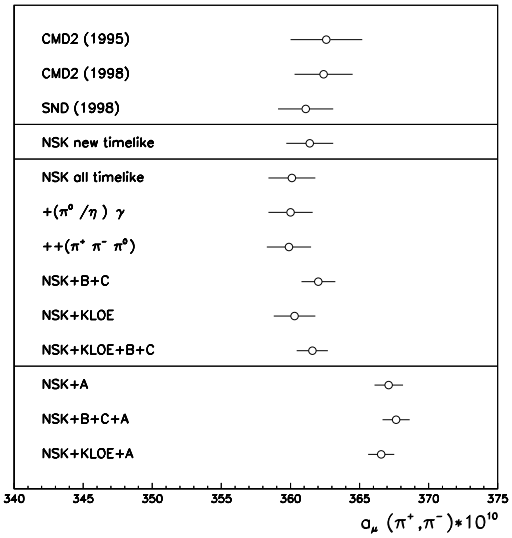


Fig. 1. The $\pi\pi$ loop contribution to $g-2$ integrated between 0.630 and 0.958 GeV using our global fit running with various combinations of data sets. "NSK" means all $e^+e^-$ annihilation channels quoted in the text.

In the (global) HLS model, the $\tau$ spectrum lineshape is essentially determined by the Higgs–Kibble $\rho^\pm$ mass (occuring in the Lagrangian) and by the $\rho^\pm$ coupling to a pion pair. The $\rho^0$ mass squared being $m^2(= ag^2f_\pi^2)$ and $g$ its coupling constant to a pion pair, we have defined the corresponding quantities for the $\rho^\pm$ meson by $m^2 + \delta m^2$ and $g + \delta g$. Interestingly, the absolute magnitude of the $\tau$ spectrum and the $\rho^\pm$ width are both determined in the HLS model by the $\rho^\pm\pi\pi$ coupling constant and, then, by $g + \delta g$. ISB effects specific of the $\tau$ decay modify this picture by introducing short range [18] ($S_{\rm EW}$) and long range [19] ($G_{\rm EM}(s)$) corrections which both factor out in the form factor expression. Therefore, these contribute in an identified way to the absolute magnitude of the $\tau$ spectrum.

We have first performed global fits with all $e^+e^-$ annihilation data[3)] and $\tau$ data in order to determine

1) See, for instance, Eq. (7) in [45].

2) As can be concluded from Figure 6 in [51], the world average value for $Br(\tau \to \pi\pi\nu_\tau)$ differs only marginally from the corresponding ALEPH [44] measurement.

3) Which include the cross sections for $e^+e^- \to \pi^0\gamma$, $e^+e^- \to \eta\gamma$ and $e^+e^- \to \pi^0\pi^+\pi^-$ beside the data for $e^+e^- \to \pi^+\pi^-$.

$\delta m^2$ and $\delta g$. It happens [15, 16] that the fits return $\delta m^2$ and $\delta g$ consistent with zero at a $\simeq 1\sigma$ level. Therefore, we do not find significant differences between the $\rho^0$ and $\rho^\pm$ (Lagrangian) masses and couplings. It thus follows that the difference between the pion form factor in $\tau$ decays ($F_\pi^\tau(s)$) and the I=1 part of the pion form factor in $e^+e^-$ annihilations ($F_\pi^e(s)$) is fully carried by the factor $\sqrt{S_{\rm EW}G_{\rm EM}(s)}$, which affects the $\tau$ dipion spectrum.

Then, fixing $\delta m^2 = \delta g = 0$, we have redone our final fits, always allowing for a rescaling of the B data sample and by varying the combination of data sets (listed in Section 4) submitted to the global fit.

## 7 A localized failure of CVC ?

Our global fits are always fairly good [15, 16] and result in an overall rescaling factor for the B form factor $1+\lambda$ with $\lambda = (-4.84^{+1.37}_{-0.92})\%$, in good correspondence with the BELLE fit result [45] which can be written $\lambda_{\rm BELLE} = -(2\pm1\pm4)\%$. In this approach, the C and B data samples are always well described ; the ALEPH spectrum is reasonably well described below 1 GeV, however more poorly than the C and B data samples [16]. This is due to having a fixed absolute normalization of ALEPH data, i.e. the presently accepted value for $Br(\tau \to \pi\pi\nu_\tau)$. Indeed, relaxing this constraint reveals that the ALEPH spectrum lineshape fits the global picture almost as well as the CLEO and BELLE spectra.

At this step, one should note that the HLS model we use, equiped with symmetry breaking schemes, accounts fairly well for :

- all $e^+e^-$ annihilation cross sections listed in Section 4,
- all partial width decays of the form $P\gamma\gamma$, $VP\gamma$ and $\eta/\eta' \to \pi^+\pi^-\gamma$,
- the lineshape of the dipion spectrum in $\tau$ decay, especially those provided by CLEO and BELLE which are quite similar.

Stated otherwise, the single piece of information which does not fit within this overall picture is the accepted absolute normalization of the $\tau$ dipion spectrum, i.e. $Br(\tau \to \pi\pi\nu_\tau)$.

If one excludes an experimental bias, one thus needs a specific additional breaking effect affecting solely the $\tau$ decay. Interestingly, this missing piece is quite consistent with a simple global rescaling of the $\tau$ spectra, as the lineshape is already well in accord with VMD expectations.

One should note at this step, a specific consequence of having included the data for $e^+e^- \to \pi^0\gamma$, $e^+e^- \to \eta\gamma$ and $e^+e^- \to \pi^0\pi^+\pi^-$ annihilations beside those for $e^+e^- \to \pi^+\pi^-$. As stated above several times, in this case, one has to withdraw the $\rho/\omega/\phi \to (\pi^0/\eta)\gamma$ decay widths from the decay mode data set considered.

Using only the $e^+e^- \to \pi^+\pi^-$ data and the $\tau$ spectra, one ends up now, as already in our [12], with a good consistency of the ALEPH spectrum – as such, with its fixed normalization – and the $e^+e^- \to \pi^+\pi^-$ data within our model framework ; this is reflected by the global fit probability, in this case larger than 70% with an ALEPH $\chi^2$ per point of $\simeq 1$.

Inspecting more carefully, the issue, one finds that introducing either $e^+e^- \to (\pi^0/\eta)\gamma$ or $e^+e^- \to \pi^0\pi^+\pi^-$ data samples dramatically breaks this agreement. In this process, if one fixes the absolute scale of the ALEPH spectrum to the world average value for $Br(\tau \to \pi\pi\nu_\tau)$, the $\chi^2$/point of ALEPH data increases to $\simeq 1.6$, revealing the absolute scale issue. Of course, fixing the absolute scale of the BELLE $|F_\pi(s)|^2$ spectrum would lead to the same conclusion.

This surprising property is certainly due to fitting the $\omega$ and $\phi$ resonance lineshapes in the cross sections. This should constrain the ISB functions $\alpha(s)$, $\beta(s)$ and $\gamma(s)$ more sharply than the $\rho/\omega/\phi \to (\pi^0/\eta)\gamma$ partial width information solely.

## 8 Influence of the $\tau$ spectra

Figure 1 displays the value for $a_\mu(\pi\pi)$ integrated along the canonical interval around the $\rho$ peak, as coming from our (global) fits. The 4 upmost data points are the values shown in Table 1. The fourth line gives the result derived from the combined fit to the data given in Refs. [25–28] also given in Table 1. The fifth line displays the result coming from the combined fit to the $\pi^+\pi^-$ data sets just quoted and to the older $\pi^+\pi^-$ data sets given in [22, 23]. For the line indicated by $+(\pi^0/\eta)\gamma$, we have added the corresponding data sets to all $\pi^+\pi^-$ data. In order to get the result indicated at the line flagged by $++(\pi^+\pi^-\pi^0)$, the corresponding data samples have been considered together with all the previous ones. Concerning the rest of Fig. 1, NSK denotes all $e^+e^-$ annilhilation data combined with KLOE, ALEPH (A), BELLE (B), CLEO (C) in the way indicated at the corresponding line.

One can conclude from Fig. 1 that all data set combinations submitted to fit and built up from all $e^+e^-$ annihilation samples and from the (rescaled) B

and C sets provide quite consistent results. Instead, as shown by the 3 downmost $a_\mu(\pi\pi)$ values, including the ALEPH data set, if not rescaled, always provides a shift upwards by $\simeq 5\ 10^{-10}$. If one allows for some freedom to its absolute scale allowed by the 0.5% uncertainty on its value for $Br(\tau \to \pi\pi\nu_\tau)$, this upward shift can be reduced to about $\simeq 3\ 10^{-10}$. However, this implies a correction to their measured value for $Br(\tau \to \pi\pi\nu_\tau)$ by about $4\sigma$.

## 9 Conclusions

We have proved that a theoretical VMD input permits to significantly improve the accuracy of predicted value for the muon $g-2$ value, as clear from Table 1. The model exhibits the full consistency of all $e^+e^-$ data sets with each other. Some further improvement, however marginal, is reached by adding the $\tau$ spectra. Our VMD input certainly increases the disagreement between the expected value for the muon $g-2$ and its direct BNL measurement.

Another important remark is that the $\rho$ meson lineshape observed in the $\tau$ dipion spectra in perfect agreement with expectations from VMD. The single surviving issue in our data set, the largest one ever analyzed within a single model, is solely the value for $Br(\tau \to \pi\pi\nu_\tau)$, expected slighly smaller than its presently accepted value. If not an experimental bias, this may indicate that symmetry breaking effects in $\tau$ decays are still to be revisited. Until this issue is clarified, one should consider cautiously the predictions for the muon $g-2$ provided by the $\tau$ dipion spectrum, especially those depending on the absolute scale of this spectrum.

### References


1 Bando M, Kugo T, Yamawaki K. Phys. Rept., 1988, **164**: 217–314
2 Harada M, Yamawaki T. Phys. Rept., 2003, **381**: 1–233
3 Fujiwara T, Kugo T, Terao H, Uehara S, Yamawaki K. Prog. Theor. Phys., 1985, **73**: 926–941
4 Wess J, Zumino B. Phys. Lett., 1971, **37**: 95–97
5 Witten E. Nucl. Phys., 1983, **B223**:422–432
6 Benayoun M, O'Connell H B. Phys. Rev. D, 1999, **58**: 074006
7 Bando M, Kugo T, Yamawaki K. Nucl. Phys. B, 1985, **259**: 493–502
8 Benayoun M, DelBuono L, O'Connell H B. Eur. Phys. J. C, 2000, **17**: 593–610
9 't Hooft G. Phys. Rept., 1986, **142**: 357–387
10 Bramon A, Grau A, Pancheri G. Phys. Lett., 1995, **344**: 240–244
11 Bramon A, Grau A, Pancheri G. Phys. Lett., 1995, **345**: 263–268
12 Benayoun M, David P, DelBuono L, Leitner O, O'Connell H B. Eur. Phys. J. C, 2008, **55**: 199–236
13 Benayoun M, DelBuono L, Eidelman S, Ivanchenko V N, O'Connell H B. Phys. Rev. D, 1999, **59**: 114027
14 Benayoun M, David P, DelBuono L, Leruste, P, O'Connell H B. Eur. Phys. J. C, 2003, **31**: 525–547
15 Benayoun M, David P, DelBuono L, Leitner O. arXiv:0907.4047 (hep–ph), 2009, accepted for publication in Eur. Phys. J. C
16 Benayoun M, David P, DelBuono L, Leitner O. arXiv:0907.5603 (hep–ph), 2009, submitted for publication in Eur. Phys. J. C
17 Bramon A, Grau A, Pancheri G, Jose Luis Lucio M. Phys. Lett. B, 2000, **486**: 406–413
18 Marciano W J, Sirlin A. Phys. Rev. Lett., 1993, **71**: 3629–3632
19 CiriglianoV, Ecker G, Neufeld H. Phys. Lett. B, 2001, **513**: 361–370
20 CiriglianoV, Ecker G, Neufeld H. JHEP, 2002, **08**: 002
21 Gounaris G J, Sakurai J J. Phys. Rev. Lett., 1968, **21**: 244–247
22 Barkov L M et al. Nucl. Phys. B, 1985, **256**: 365–384
23 Quenzer A et al. Phys. Lett. B, 1978, **76**: 512–516
24 Aulchenko V M et al. Phys. Lett. B, 2002, **527**: 161–172
25 Akhmetshin R R et al. Phys. Lett. B, 2004, **578**: 285–289
26 Akhmetshin R R et al. Phys. Lett. B, 2007, **648**: 28–38
27 Akhmetshin R R et al. JETP Lett., 2006, **84**: 413–417
28 Achasov M N et al. J. Exp. Theor. Phys., 2006, **103**: 380–384
29 Akhmetshin R R et al. Phys. Lett. B, 1999, **460**: 242–247
30 Akhmetshin R R et al. Phys. Lett. B, 2005, **605**: 23–36
31 Achasov M N et al. Eur. Phys. J. C, 2000, **12**: 25–33
32 Achasov M N et al. Phys. Lett. B, 2003, **559**: 171–178
33 Achasov M N et al. Phys. Rev. D, 2007, **76**: 077101
34 Akhmetshin R R et al. Phys. Lett. B, 1995, **364**: 199–206
35 Akhmetshin R R et al. Phys. Lett. B, 1995, **434**: 426–436
36 Akhmetshin R R et al. Phys. Lett. B, 2006, **642**: 203–209
37 Achasov M N et al. Phys. Rev. D, 2003, **68**: 052006
38 Achasov M N et al. Phys. Rev. D, 2002, **66**:032001
39 Dolinsky S I et al. Phys. Rept., 1991, **202**: 99–170
40 Barkov L M et al. BudkerINP preprint, 1989, 89-15, Novosibirsk
41 Cordier A et al. Nucl. Phys. B, 1980, **172**: 13
42 Ambrosino F et al. Phys. Lett. B, 2009, **670**: 285–291
43 Anderson S et al. Phys. Rev. D, 2000, **61**: 112002
44 Schael S et al. Phys. Rept., 2005, **421**: 191–284
45 Fujikawa M et al. Phys. Rev. D, 2008, **78**: 072006
46 Grayer G et al. Nucl. Phys. B, 1974, **75**: 189–245
47 Colangelo G. Nucl. Phys. Proc. Suppl., 2004, **162**: 185–191
48 Colangelo G. Nucl. Phys. Proc. Suppl., 2006, **162**: 256–259
49 Colangelo G, Private Communication
50 Amsler C et al. Phys. Lett. B, 2008, **667**: 1–1340
51 Davier M et al. arXiv:0907.5603, (hep–ph), 2009, submitted for publication in Eur. Phys. J. C
52 Venanzoni G et al. arXiv:0906.4331, (hep–ex), 2009
53 Davier M et al. arXiv:0908.4300, (hep–ph), 2009